ORIGINAL RESEARCH ARTICLE



Metallographic Investigations of a Roman Fibula from Carnuntum, Austria

Roland Haubner¹ · Angelina Pronina¹ · Susanne Strobl¹

Received: 19 November 2024 / Revised: 4 April 2025 / Accepted: 4 May 2025 / Published online: 30 May 2025 © The Author(s) 2025

Abstract

In the 1950 s a Roman fibula head was found in Carnuntum and presently examined by metallography. 3D digital microscopy (3D-DM) was used to show the ornaments on the surface. Due to the complexity of the fibula head, a micro-computed tomography (CT) was carried out. The CT scan already showed that the fibula head consisted of at least four individual pieces. Subsequently the fibula part was cold embedded under vacuum and then prepared for further metallographic investigations. Light optical microscope (LOM) and scanning electron microscope (SEM) with energy-dispersive X-ray analysis (EDS) were used. The investigations showed that not less than four different copper alloys were used for the fibula head. The bronze alloys are very different, which suggests the use of various starting materials including recycled copper alloys. The microstructure of the bronzes is uniform and—depending on their compositions—contains precipitates like Pb and the intermetallic phase Cu₄₁Sn₁₁. The corrosion layers exhibit a pronounced Sn enrichment and contain most likely malachite as well as locally both cuprite and azurite. On some surfaces, textile fibers were embedded in the corrosion layer, which indicate that a textile fiber was in contact with the fibula during corrosion.

Keywords Bronze · Fibula · Romans · Carnuntum · Metallography

Introduction

A fibula is a brooch for fixation of garments and is functionally equivalent to today's safety pins. A fibula had a practical function of fastening clothing and is additionally used for decorative purposes. The first fibulae are known from the late Bronze Age. Later they were used throughout the Hall-statt period, La Tène period, the Roman Imperial period, and

This invited article is part of a special topical issue of the journal *Metallography, Microstructure, and Analysis* on Archaeometallurgy. The issue was organized by Dr. Patricia Carrizo, National Technological University—Mendoza Regional, Dr. Omid Oudbashi, University of Gothenburg, Mr. Joseph Paul Mitchell, Avedis Zildjian Company, and Prof. Joshua Mueller, Michigan Technological University, on behalf of the ASM International Archaeometallurgy Committee.

- ⊠ Roland Haubner roland.haubner@tuwien.ac.at
- Susanne Strobl susanne.strobl@tuwien.ac.at
- ¹ Institut für Chemische Technologien und Analytik, Technische Universität Wien, Getreidemarkt 9/164-03, A-1060 Vienna, Austria

in the early Middle Age. They were used by both sexes and had different significance, depending on the type of society and thus, a lot of different types are known [1–3]. Fibulae were made of bronze or iron and different materials were used for decoration, e. g. almandine, glass, enamel.

Bronze fibulae were made by casting of appropriate alloys and subsequently fine-forged. All available raw materials, including recycled material, were used for the alloys. This circumstance results in very different compositions of the used alloys [4–8].

During the Roman Empire period, fibulae were also an important part of the wardrobe. Due to the enormous dimension of the Roman Empire, the Celtic as well as provincial Roman influences, a lot of different fibula types are known [9–13].

The head of a Roman fibula which was found in Carnuntum in the 1950 s is shown in (Fig. 1). It was not possible to find an identical fibula in literature. Striking are the head plate above the spiral (Fig. 1a, c, d), the hole in the bow (Fig. 1b), and the end caps (Fig. 1b, d).

Based on its appearance, it is a high profiled fibula. According to Almgren [9], it should be classified in group IV, no. 73.



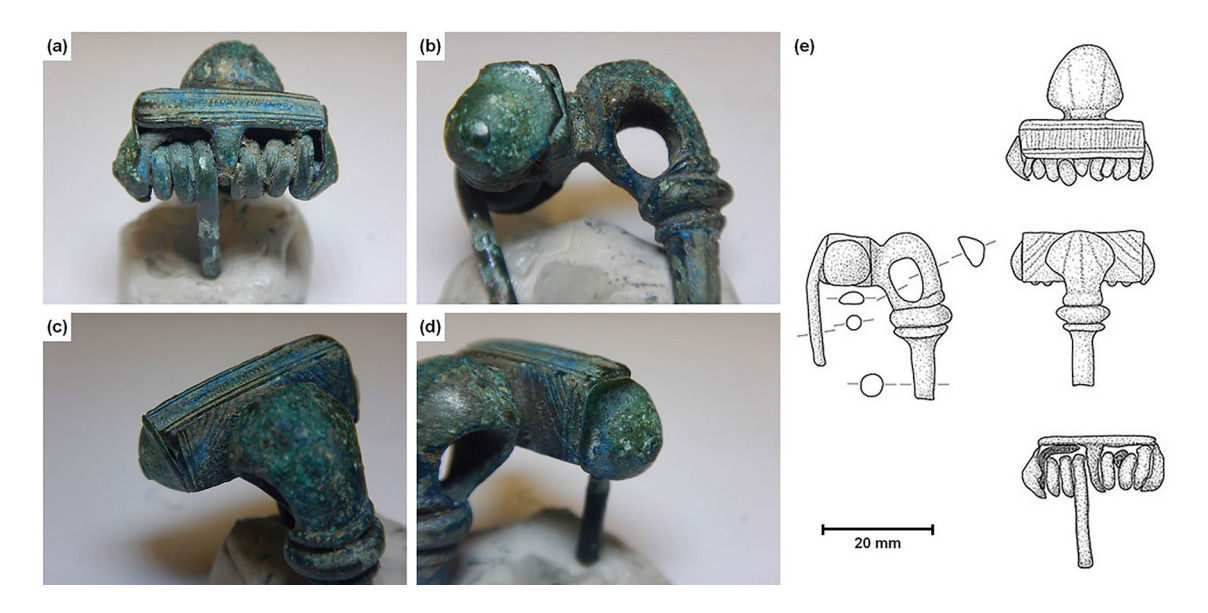


Fig. 1 Photos of fibula head. a-d various directions; e drawing

Jobst [13] classified it as high profiled fibula with support plate. Variant C: A70 was used between the end of the 1st and the beginning of the 2nd century AD. Variant D: A73 was used in the middle of the 2nd century AD.

Experimental Procedures

The fibula head was first examined by nondestructive methods using micro-computed tomography (micro-CT) (VISCOM X8060) and 3D digital microscopy (3D-DM) (KEYENCEVHX-5000).

Since conventional metallography with cutting and metallographic preparation was not possible for this object, it was vacuum cold mounted. After a cut with a precision cutting machine, the fibula head was embedded again. The metallographic preparation and documentation took place in several stages. After plane grinding polishing was carried out with 9, 3, and 1 µm diamond suspensions. Klemm 2 solution was used to develop the microstructure [14]. Light optical microscope (LOM) (Olympus GX51 with an associated CCD camera) and scanning electron microscope (SEM) (company FEI) with backscattered electron mode (BSE) and energy-dispersive X-ray analysis (EDS) (company EDAX) were used for the investigations. The SEM worked in low vacuum mode to avoid charging. The selected acceleration voltage for the electrons was 20 kV.

Results and Discussion

The fibula head is shown in Fig. 1 from various directions. The dimensions are 28 x 30 x 24 mm. The surface is covered with a greenish-bluish patina. The bow and the pin are broken. One of the end caps was lost during handling.

Nondestructive Investigation Methods

In order to document the internal structure of the fibula, micro-CT examinations were carried out. From the obtained data, two orientations were calculated and selected sections are shown in Fig. 2 and 3. In Fig. 2 you can see cuts from the front side with the pin toward the back where the bow is located. It is easy to notice that the pin merges into the spiral (Fig. 2b), which was a wire coiled around an arbor (Fig. 2c) and subsequent an end cap is fixed at the arbor. The head plate above the spiral (Fig. 2d) and the support plate are also visible (Fig. 2e). At the transition from the support plate to the bow and also in the bow itself, there are no irregularities visible. This means that it is one piece (Fig. 2e–h). In the side view, the arbor, wrapped by the spring spiral, can be clearly seen at



Fig. 2 Micro-CT measurements. CT sections from the front to the back

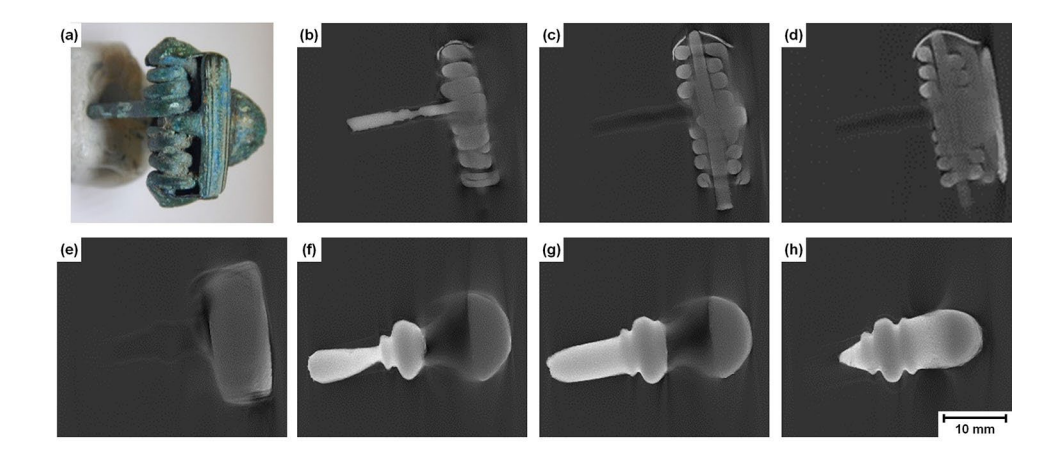


Fig. 3 Micro-CT measurements. CT sections from the side view

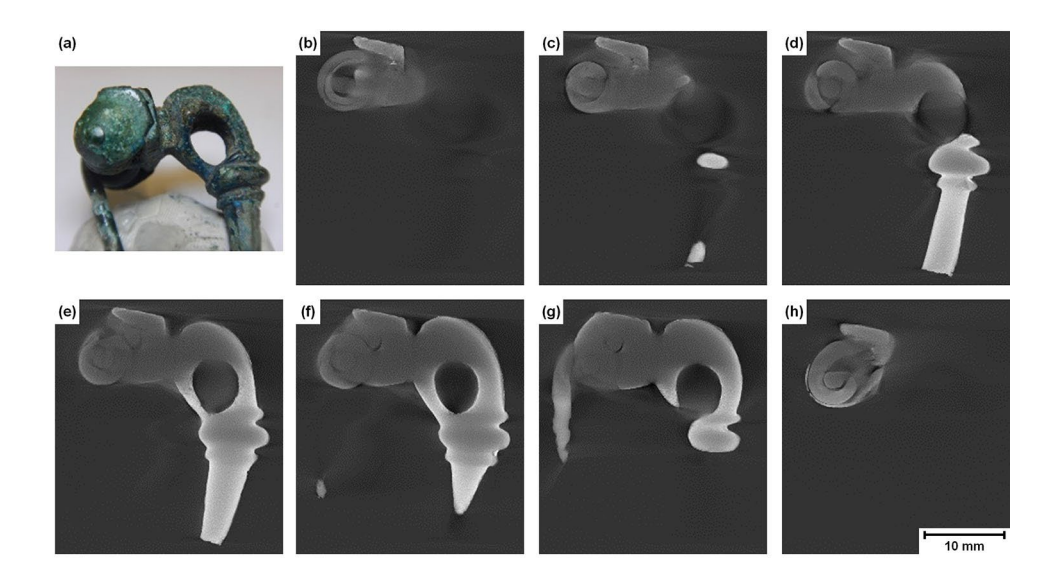


Fig. 4 3D-DM pictures to show the decoration, the patina, and fibers fixed in the patina



both ends (Fig. 3b, c, h). The middle section shows the bow with the transition to the support and the head plate (Fig. 3d-g).

A decoration can be seen on the surface of the head plate (Fig. 4a-c). Two longitudinal grooves and in-between a pattern of diagonal lines can be observed (Fig. 4b, c). The



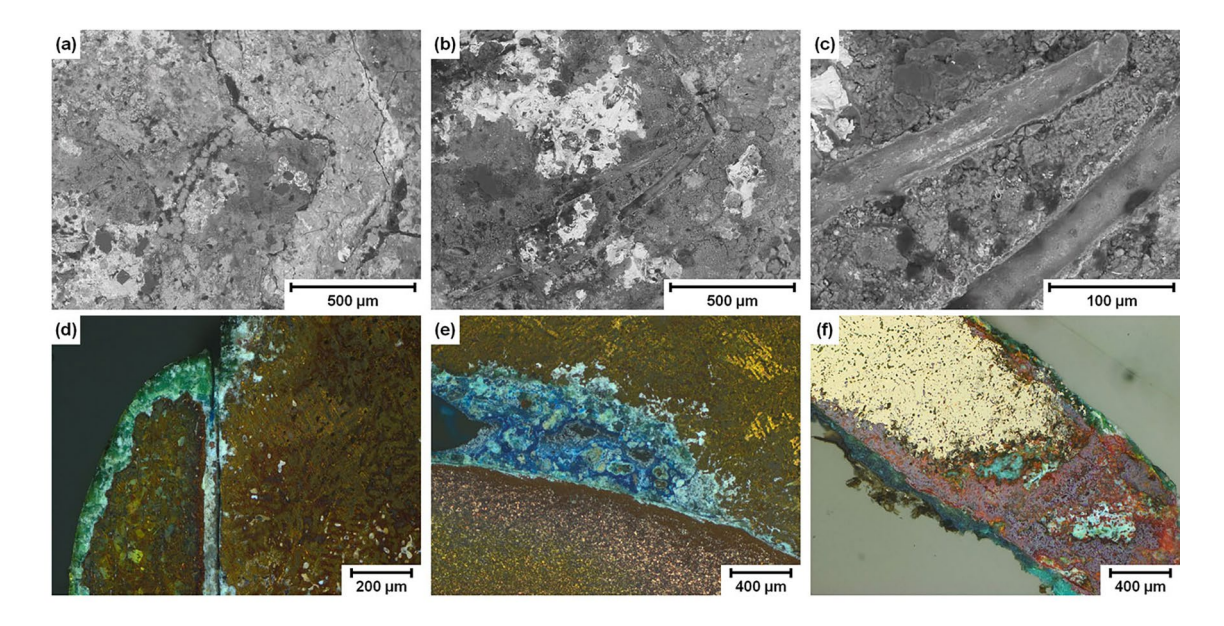
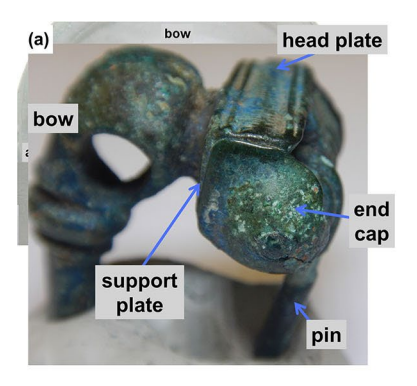
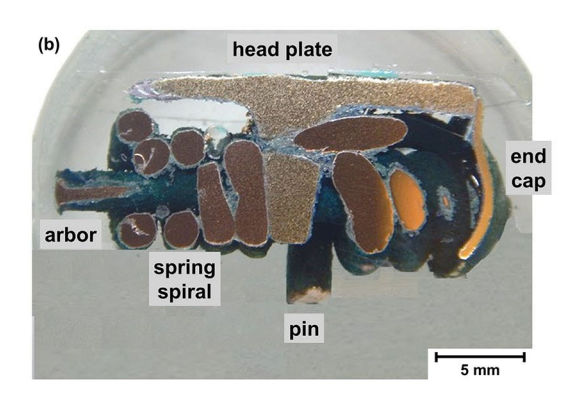


Fig. 5 Corrosion products on the fibula. a-c surface in SEM, d-e metallographic cuts with typical corrosion products in LOM, polarized light

Fig. 6 Total view of the fibula, a description of the different parts, **b** metallographically prepared fibula head





patina is green, which most likely corresponds to the mineral malachite $(Cu_2(CO_3)(OH)_2)$, and partly blue, which most likely corresponds to the mineral azurite $(Cu_3(CO_3)_2(OH)_2)$ (Fig. 4b–f). Fibers can be seen additionally on the surface, which probably come from a textile which was in contact with the fibula (Fig. 4d, e). The fibers were fixed to the surface by corrosion products. In SEM-BSE bright areas can be seen on the surface which contain Pb-enriched corrosion products (Fig. 5a, b). Elongated stripes can be observed additionally, which correspond to the textile fibers (Fig. 5c). The various corrosion products of copper are clearly visible in metallographic sections: They are most likely, green malachite $(Cu_2(CO_3)(OH)_2)$ (Fig. 5d), blue azurite $(Cu_3(CO_3)_2(OH)_2)$ (Fig. 5e), red cuprite (Cu_2O) (Fig. 5f).

Metallographic Investigations

Cuts were made in different directions, and the samples were prepared by metallographic techniques. In a cut through the

Table 1 SEM-EDS results of the different copper alloys found in the fibula. Mean values of several area measurements (wt.%) (ldl = lower detection limit)

	Bow	Pin	Arbor	End cap
Cu	77.7	96.6	92.5	85.4
Sn	6.0	2.4	4.1	5.2
Pb	7.3	0.2	1.6	0.3
Zn	8.8	ldl	1,8	8.2
S	0.2	0.8	ldl	0.8

entire fibula head, all parts of the fibula were exposed and were accessible for metallographic examinations (Fig. 6). The individual fibula parts and their alloys are described below.

SEM-EDS results of the different materials are summarized in Table 1. Since the alloys are partially inhomogeneous, average values were calculated from several surface



measurements. It is not possible to detect trace elements, especially if they are inhomogeneous distributed [15, 16]. However, it is clear from the measured values that the alloy compositions are very different.

The Bow, Support Plate, and Head Plate

Based on the micro-CT images, one can deduce that bow, support plate, and head plate are one single piece, since no joints are visible (Figs. 2, 3). A section through the head plate shows a uniform cast structure (Fig. 7a). The SEM-EDS analysis for this alloy showed 77.7 wt% Cu, 6 wt%

Fig. 7 Section through the head plate (LOM, Klemm 2 etched). a overview, **b**–**d** various magnifications

Sn, 7.3 wt% Pb, 8.8 wt% Zn, and 0.2 wt% S (Table 1). This composition could be classified as gunmetal, which was widely used in the Roman Empire [17, 18].

You can distinguish black Pb precipitations and the bright bluish phase $Cu_{41}Sn_{11}$ which is formed at the eutectoid point in the Cu-Sn phase diagram. First, the dark brown areas with less Sn were formed during solidification (Fig. 7b–d). The fact that the dendritic structure is not clearly visible could be due to subsequent deformation by fine forging. It cannot be determined whether the decorations on the surface were introduced during casting or by

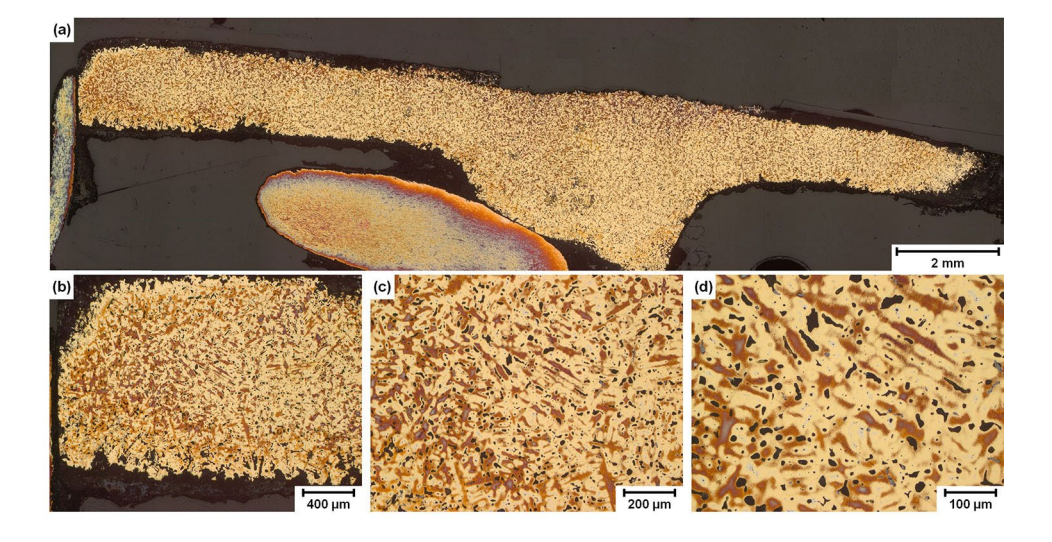
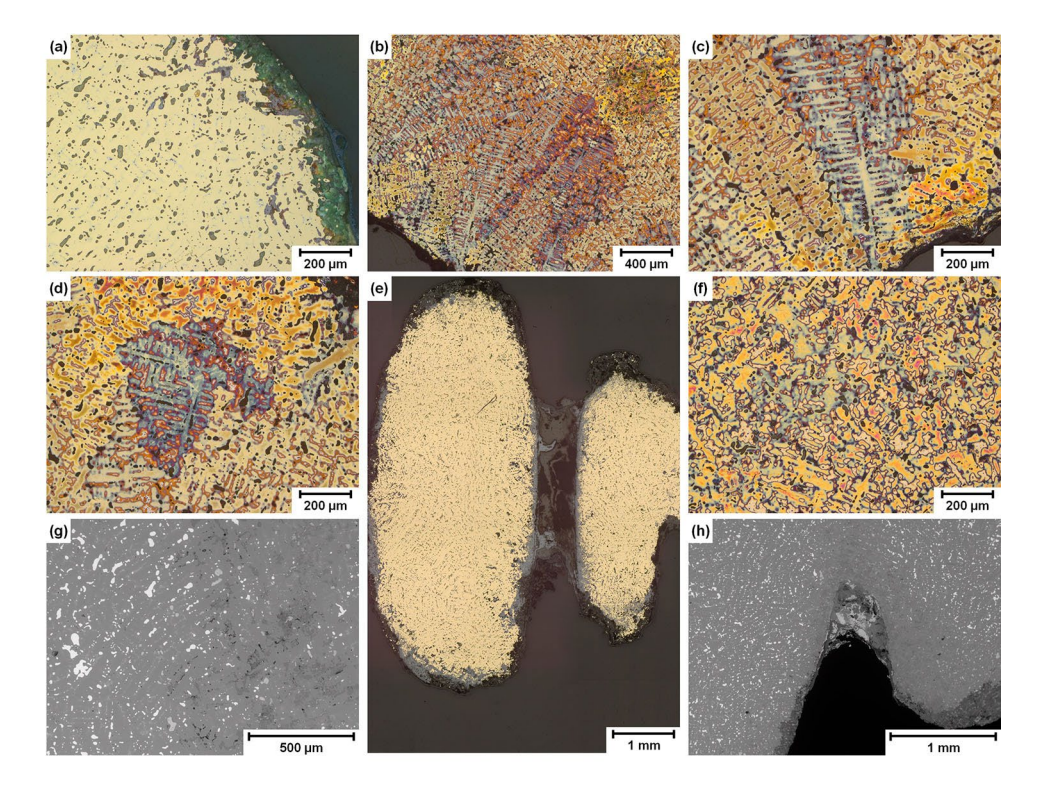


Fig. 8 Microstructure in the region of the support plate and bow (LOM). a polished, polarized light, b-d Klemm 2 etched. Cross section through the bow. e overview polished, f Klemm 2 etched, g, h SEM





further processing which results in deformation. In any case, deformation twins were not observed.

The dendritic solidification structure is clearly visible in the area of the support plate as well as in the transition to the bow (Fig. 8a–d). The cell structure originated by dendritic solidification, above the peritectic transformation, is clearly visible (Fig. 8c, d) [19, 20]. Here the patina on the surface consists of malachite (Fig. 8a) [21, 22].

The cast structure of the bronze is also present in wide parts of the bow and the beads (Fig. 8e, f). Lead containing corrosion products can be found in the recesses between the rings (Fig. 8g, h). After further material removal, no joint could be found. This is conform to the results of the CT examinations.

A SEM-EDS element distribution clearly shows the distribution of the individual elements in the cast structure (Fig. 9). Sn is enriched in the intermetallic phase Cu₄₁Sn₁₁, somewhat is in the interdendritic areas and rarely it is found in the dendrites, which solidify firstly.

Zn is homogeneously distributed in Cu. Pb, which is insoluble in Cu, solidifies at last, and is found in the interdendritic areas. S is associated with Zn (ZnS), but also with Pb. ZnS was also confirmed by SEM-EDS point measurements. It cannot be determined if PbS is present, since Ni, P, and As are also associated with Pb.

The Spring Spiral, Pin

Spiral and pin were also made in one piece. For this purpose, a wire with a diameter of about 1.5 mm was produced, which was then coiled around the arbor. Longitudinal sections and cross sections of the wire can be seen in Fig. 10. The SEM-EDS analysis showed 96.6 wt% Cu, 2.4 wt% Sn, 0.2 wt% Pb, and 0.8 wt% S (Table 1). This alloy has a high copper content. Thus, no precipitations are observed in the structure, which elongated shape would indicate deformation (Fig. 10a, b). The longitudinal sections show a uniform structure with grain sizes up to 10 µm in diameter. Many of the grains contain straight-aligned twin grain boundaries, which are difficult to see due to the low magnification (Fig. 10c). In the cross sections of the wire, both cracks and deformation patterns can be seen (Fig. 10d, f-h). The large cracks had probably developed during wire production, because the deformation structures can be found near the cracks (Fig. 10d, g, h). Furthermore, the cracks are filled with corrosion products.

In the straight part of the pin, corrosion products are present on the surface, which indicate pitting corrosion. The corrosion zones are layered with Cu₂O in contact with the metal and malachite at the rim (Fig. 11a–c). In the longitudinal section, elongated structures of different colors are visible, which can be attributed to the deformation during production (Fig. 11d–f). Otherwise small inclusions are visible

Fig. 9 SEM-EDS element distribution. Dendritic casting microstructure in the region of the bow

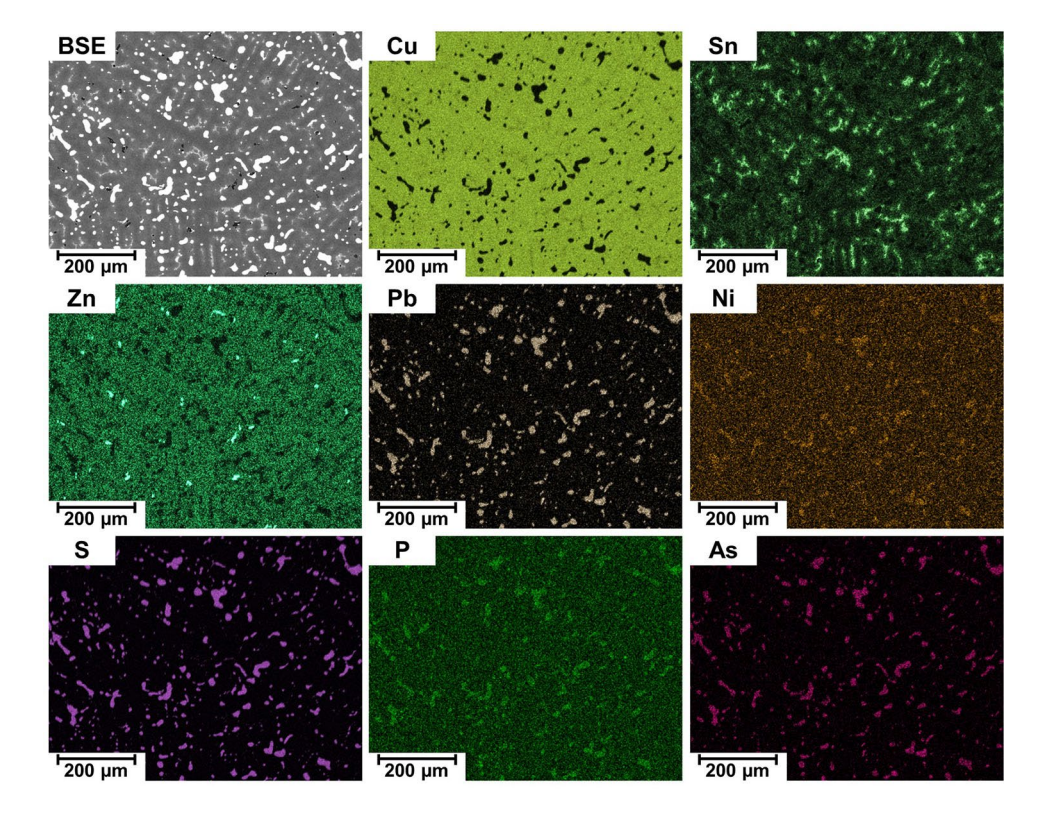
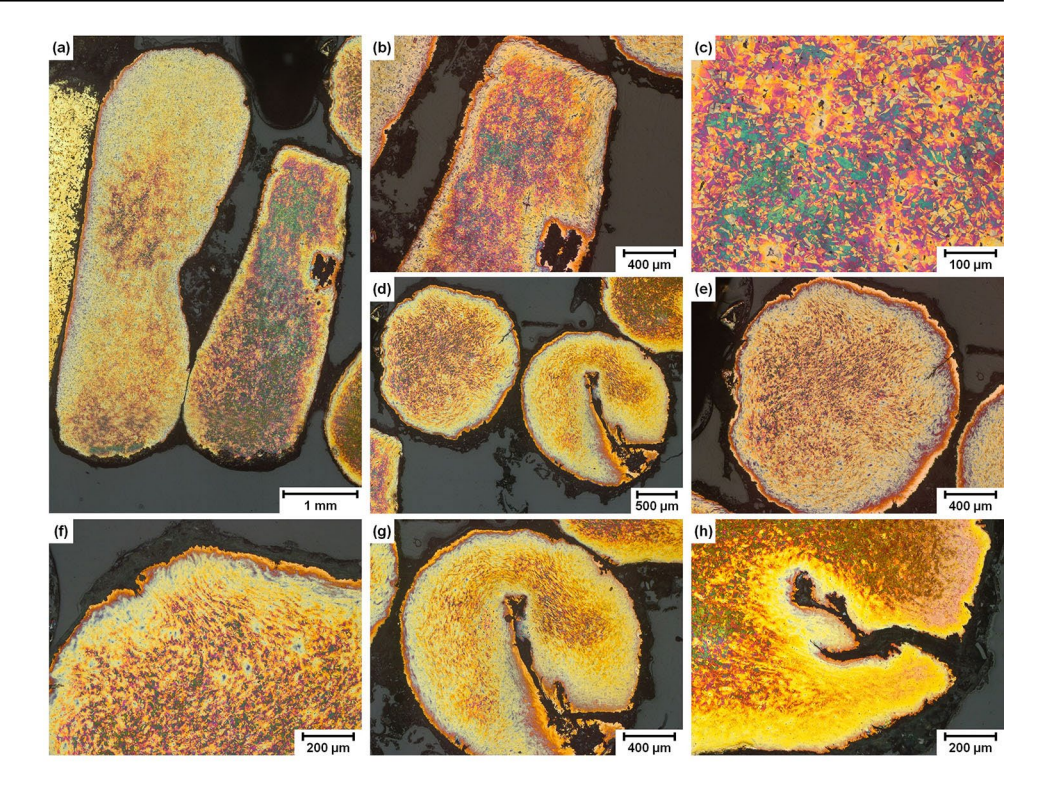




Fig. 10 Various cross sections through the wire of the spiral (LOM, Klemm 2 etched). a–c longitudinal cuts, d–h vertical cuts



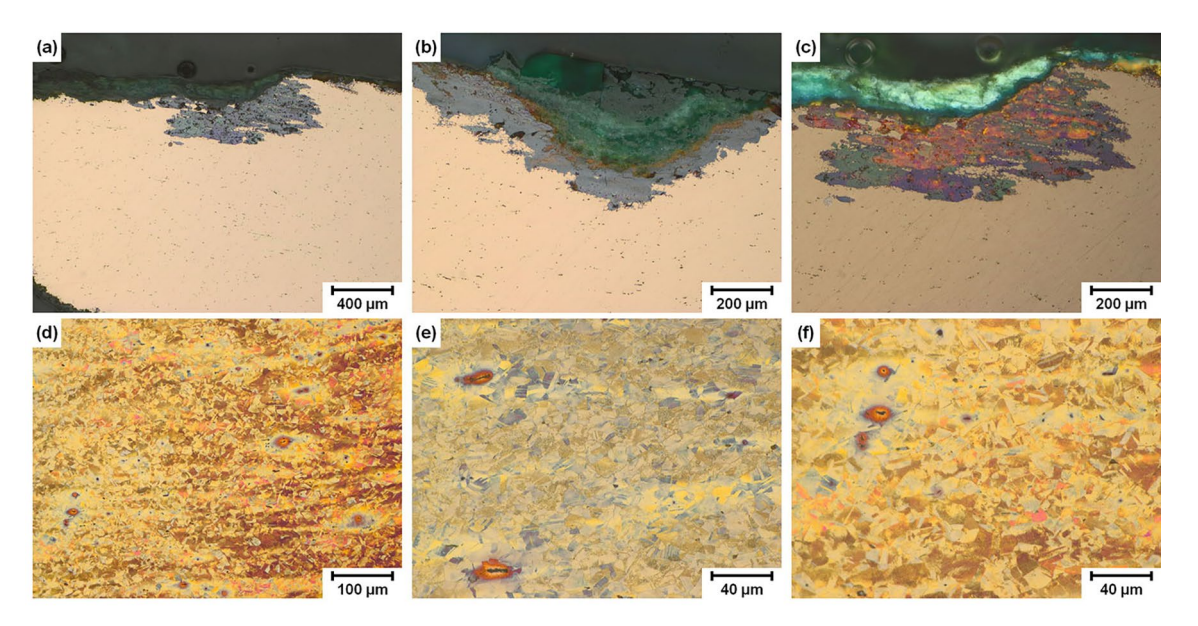


Fig. 11 Microstructure of the straight part of the pin (LOM). a-c corrosion products, d-f microstructure after Klemm 2 etching

in the homogeneous structure. As before, in the spiral area the maximum grain size is about $10~\mu m$.

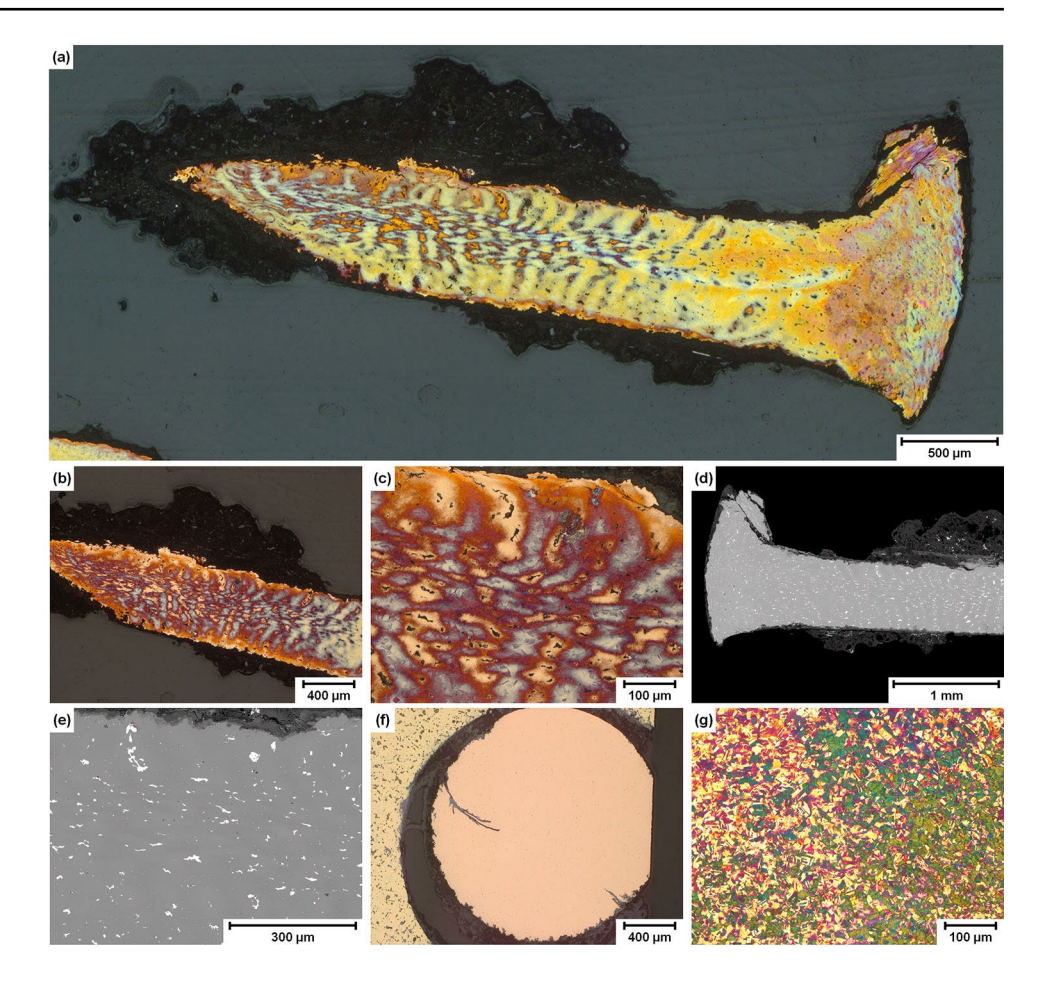
The Arbor

The arbor passes through the fibula head and fixes the spiral and the end caps. The SEM-EDS analysis showed 92.5 wt% Cu, 4.1 wt% Sn, 1.6 wt% Pb, and 1.8 wt% Zn (Table 1).

In the longitudinal section, a thickened end can be seen on one side, which can be explained by the installation of the end cape (Fig. 12a). Unfortunately, the end cape cannot be seen here because it has been lost. In the round part of the arbor, clear signs of deformation are visible, which are due to the shaping of the material (Fig. 12b, c). The black precipitations in the LOM correspond to Pb, and the color shades from dark brown to light brown are



Fig. 12 Microstructures of the arbor. a overlook LOM, Klemm 2 etched. b, c LOM, Klemm 2 etched. d, e SEM. f LOM, polished, g LOM, Klemm 2 etched



caused by Sn segregation during solidification. In SEM Pb appears white and the elongated structure is due to deformation (Fig. 12d, e). A cross section shows a very homogeneous structure but cracks that reach a length of about 0.5 mm (Fig. 12f, g). The structure is recrystallized and fine-grained, with a grain size of about 10 μ m, and has numerous twins (Fig. 12g).

The End cap

The end cap is a convex metal plate, approximately 0.4 mm thick, and in its center is attached to the arbor (Fig. 2c). The SEM-EDS analysis for this alloy showed 85.4 wt% Cu, 5.2 wt% Sn, 0.3 wt% Pb, 8.2 wt% Zn, and 0.8 wt% S (Table 1). The end cap is also fixed to the head plate using solder (Fig. 13a, b). The sheet has elongated inclusions, which had formed during production by fine forging (Fig. 13c, d), and its structure is very uniform. In SEM, the inclusions are partly white (Pb) and predominantly dark gray (Cu₂O) (Fig. 13e–g). Cu₂O was confirmed by SEM-EDS point measurements. The surface is covered with a uniform patina [23].

The Solder

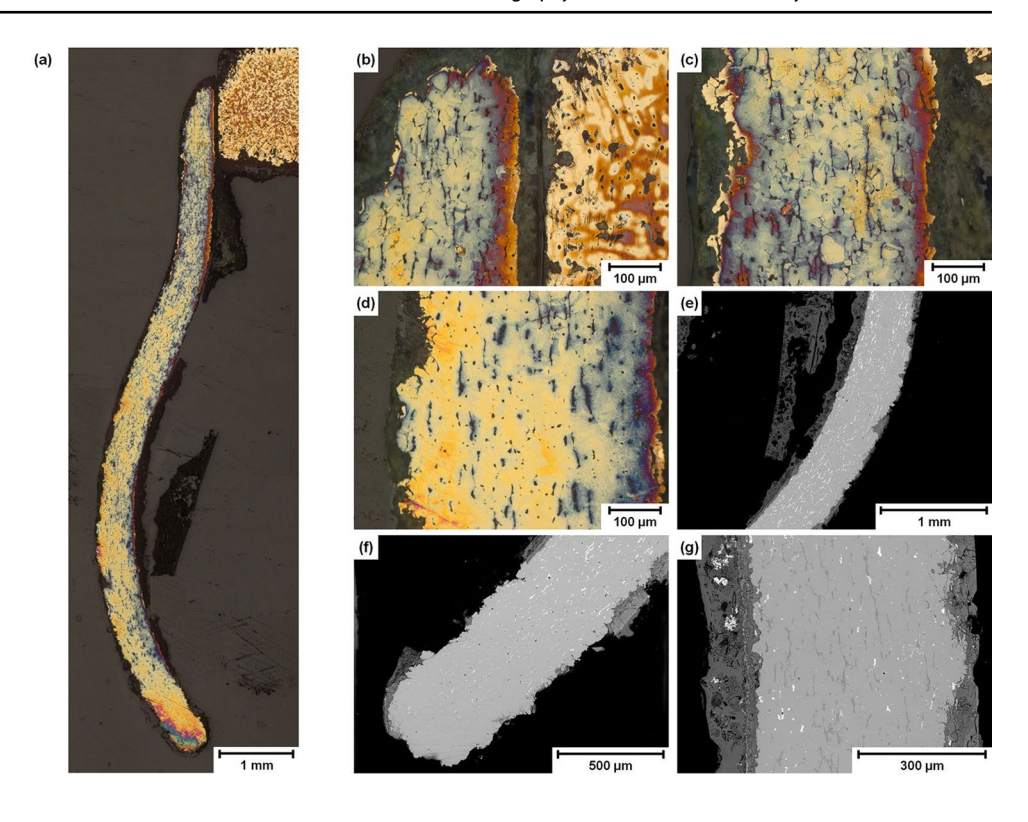
Solder was found in some places on the brooch but mainly in the area of the head plate, the end cap, and between the coils of the spiral (Fig. 14). Table 2 summarizes only vague analysis results, since exact measurements were not possible due to the mixing of solder with corrosion products. The solder consists dominantly of Pb, although small concentrations of Sn, As, S, and P were measured. O, C, Cl, and Cu were introduced by the corrosion process.

It is noticeable that in areas with corroded solder azurite is increasingly present as a corrosion product (Fig. 14a). Due to the Cl content in these areas, it can be assumed that $PbCl_2$ is a corrosion product [24] but cerussite ($PbCO_3$) is also possible.

When soldering the head plate to the end cap, it looks like a drop of solder has formed and ran downward (Fig. 14b, c). A SEM-EDS element distribution was measured from this area (Fig. 15). It is clearly visible that Pb and O are enriched in the solder regions, but small amounts of Pb were found additionally in the head plate. The phenomenon that Sn is enriched at the surface of the bronze can be attributed to corrosion, since Sn accumulates in the corrosion products.



Fig. 13 Microstructures of the end cap. a overlook LOM, Klemm 2 etched. b–d LOM, Klemm 2 etched. e–g SEM



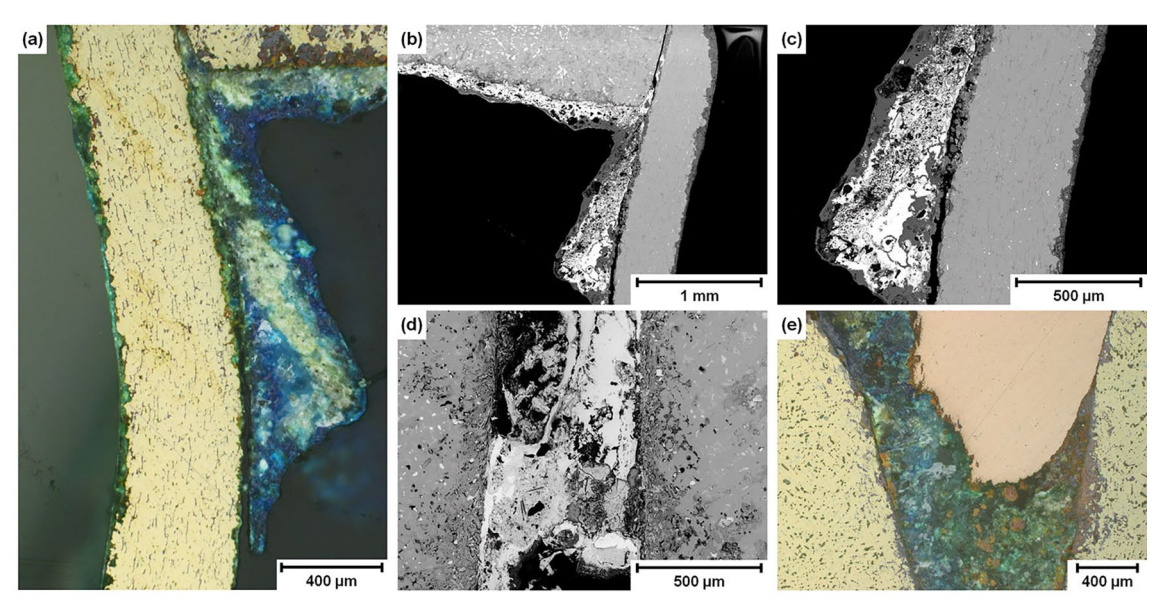


Fig. 14 Solder between head plate and end cap. a, e LOM, polarized light, Klemm 2 etched. b-d SEM

Table 2 SEM-EDS results of measurements on solders. Mean values of several area measurements (wt.%)

	Solder
С	10,4
O	16,3
Cl	3,1
Cu	7,4
Pb	61,7
Sn, As, S, P	< 0,1

Two further locations with solder and corrosion products can be seen in Fig. 14d, e. The SEM-EDS element distribution also included the elements P, As, S, and Cl. All of these elements are enriched in the Pb solder as well as in corrosion products (Fig. 16).



Fig. 15 SEM-EDS element distribution in the area of the join between the head plate and the end cap

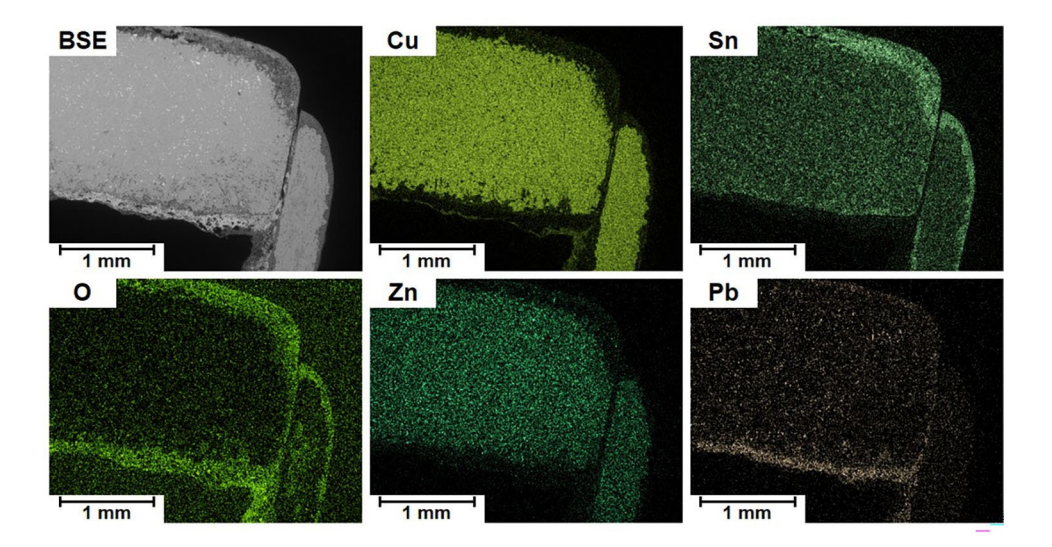
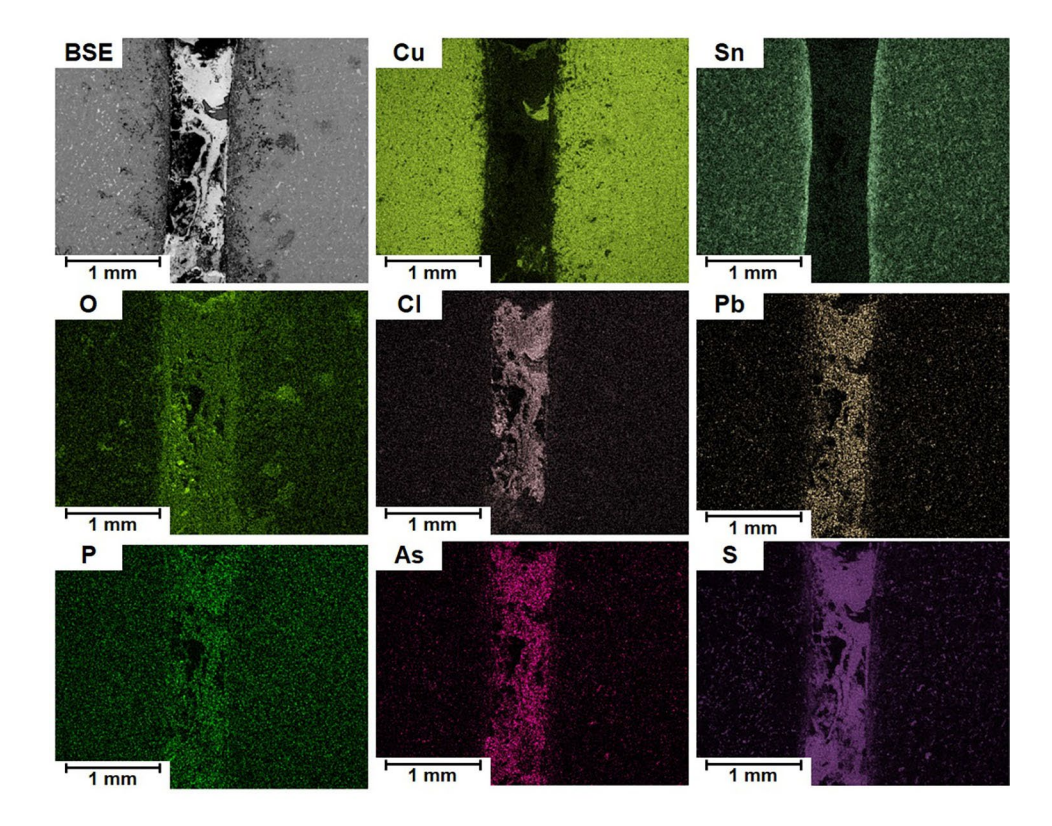


Fig. 16 SEM-EDS element distribution of an area with solder on the bow



Conclusions

The head of a Roman fibula was examined by metallography. The complexity of the fibula head could be documented by micro-computed tomography (CT). The CT scan already showed that the fibula head consisted of at least five individual pieces. Bow, support plate, and head plate formed one unit, spring spiral, and pin another. Arbor and the two end caps were individual parts.

All four components were made of different copper alloys. The bow was most different alloyed and was manufactured by casting together with support plate and head plate.

For the spring spiral and the pin, a wire from an alloy with a high copper content was used and then coiled around an arbor which was manufactured from a small rod. Finally, on both sides of the arbor end cups were fixed.



Pb as well as its corrosion products were found at various locations on the fibula head and served apparently as solder to increase the stability of the fibula.

A special feature is that azurite was found as a corrosion product, and on some surfaces, textile fibers were embedded in the corrosion layer.

Funding Open access funding provided by TU Wien (TUW).

Open Access This article is licensed under a Creative Commons Attribution 4.0 International License, which permits use, sharing, adaptation, distribution and reproduction in any medium or format, as long as you give appropriate credit to the original author(s) and the source, provide a link to the Creative Commons licence, and indicate if changes were made. The images or other third party material in this article are included in the article's Creative Commons licence, unless indicated otherwise in a credit line to the material. If material is not included in the article's Creative Commons licence and your intended use is not permitted by statutory regulation or exceeds the permitted use, you will need to obtain permission directly from the copyright holder. To view a copy of this licence, visit http://creativecommons.org/licenses/by/4.0/.

References

- R. Müller, H. Steuer, Fibel und Fibeltracht, Reallexikon der Germanischen Altertumskunde, De Gruyter, (2011)
- 2. C. Rau, Die Fibeln Europas Band 1 Von der Bronzezeit bis zur Hallstattzeit, Publisher Epubli (2021)
- 3. C. Rau, Die Fibeln Europas Band 2 Von der Latènezeit bis zum Ende des Weströmischen Reiches, Publisher Epubli (2024)
- R. Haubner, Die prähistorische kupfermetallurgie—allgemeine betrachtungen. BHM Berg- Huettenmaenn. Monatsh. 166, 343– 351 (2021). https://doi.org/10.1007/s00501-020-01056-0
- R. Haubner, S. Strobl, Microstructure of an extraordinary Bronze Age copper ingot with a high antimony content. Pract. Metallogr. 59, 732–748 (2022). https://doi.org/10.1515/pm-2022-1004
- R. Haubner, F. Ertl, S. Strobl, Examinations of a Bronze ingot made of fahlore. Practical Metallography. 54, 107–117 (2017). https://doi.org/10.3139/147.110446
- R. Haubner, S. Strobl, Investigations on copper cast cakes, sickle fragments and a spout axe of the hoard find from drassburg/burgenland. Metallogr., Microstruct., Anal. 12, 187–201 (2023). https://doi.org/10.1007/s13632-023-00936-4
- R. Haubner, S. Strobl, M. Thurner, H. Herdits, Ein Kupfergusskuchen mit hohem Antimongehalt aus Velem/Westungarn. BHM Berg Huettenmaenn. Monatsh. 165, 453–460 (2020). https://doi.org/10.1007/s00501-020-01017-7
- 9. O. Almgren, Studien über Nordeuropäische Fibelformen der ersten nachchristlichen Jahrhunderte mit Berücksichtigung der

- provinzialrömischen und südrussischen Formen, Stockholm: Haeggström (1897)
- W. Jobst, Römische Silberfibeln aus Lauriacum. Jahrb. des Oberösterr. Musealvereines. 118, 75–88 (1973)
- 11. E. Patek, Verbreitung und Herkunft der Römischen Fibeltypen Von Pannonien, The Journal of Roman Studies, 314 (1942)
- 12. E. Riha: *Die römischen Fibeln aus Augst und Kaiseraugst*, Forschungen in Augst, Band 3 (1979)
- W. Jobst, Die römischen Fibeln aus Lauriacum, Forschungen in Lauriacum. Band 10. (1975).
- G.F. Vander Voort, Metallography Principles and Practice, ASM International, 3rd printing, (2004) https://doi.org/10.31399/ asm.hb.v09.a0003752
- R. Haubner, For THEY do not know what THEY are doing. Pract. Metallogr. 60, 331–342 (2023). https://doi.org/10.1515/pm-2023-0027
- R. Haubner, Kritische Betrachtungen zur Zusammenarbeit von Archäologen und Naturwissenschaftlern. Archäol. Denkmalpfl. 4, 1–17 (2023)
- A. Jouttijärvi, Roman alloying practice. Mater. Manuf. Process. 32(7–8), 813–826 (2017). https://doi.org/10.1080/10426914.2017. 1279325
- J. Bayley, S. Butcher, Roman brooches in Britain: a technological and typological study based on the richborough Collection (The Society of Antiquaries, London, 2004)
- R. Haubner, S. Strobl, Metallography on a sickle fragment from the Drassburg/Burgenland hoard find. Pract. Metallogr. 59, 749– 760 (2022). https://doi.org/10.1515/pm-2022-1005
- R. Haubner, S. Strobl, J. Leskovar, Examinations on small bronze items from the Hallstatt period burial ground at Mitterkirchen in Upper Austria. Pract. Metallogr. 61, 630–641 (2024). https://doi. org/10.1515/pm-2024-0062
- R. Haubner, S. Strobl, P. Trebsche, Analysis of Urnfield period bronze droplets formed during casting. Mater. Sci. Forum. 891, 41–48 (2017). https://doi.org/10.4028/www.scientific.net/MSF. 891 41
- R. Haubner, Garment buttons from a Hallstatt period tumulus. Pract. Metallogr. 60, 276–288 (2023). https://doi.org/10.1515/ pm-2022-1021
- J. Pechtl, S. Strobl, R. Haubner, Ein Kupferbeil aus der frühen Kupferzeit vom Heuberg bei Ohlstadt. Deutschl., BHM Berg- und Hüttenmänn. Monatsh. 168, 406–413 (2023). https://doi.org/10. 1007/s00501-022-01310-7
- S. Pronina, R. Strobl, Haubner, Eine stark korrodierte Römische Münze aus Kupfer-Blei von Carnuntumn. BHM Berg- Huettenmaenn. Monatsh. 169, 490–496 (2024). https://doi.org/10.1007/ s00501-024-01503-2

Publisher's Note Springer Nature remains neutral with regard to jurisdictional claims in published maps and institutional affiliations.

